The MODY1 gene *HNF-4α* regulates selected genes involved in insulin secretion

Rana K. Gupta,[1,2] Marko Z. Vatamaniuk,[1,2] Catherine S. Lee,[1,2] Reed C. Flaschen,[1,2] James T. Fulmer,[1,2] Franz M. Matschinsky,[2,3] Stephen A. Duncan,[4] and Klaus H. Kaestner[1,2]

[1]Department of Genetics, [2]Institute for Diabetes, Obesity, and Metabolism, and [3]Department of Biochemistry and Biophysics, University of Pennsylvania School of Medicine, Philadelphia, Pennsylvania, USA. [4]Department of Cell Biology, Neurobiology and Anatomy, Medical College of Wisconsin, Milwaukee, Wisconsin, USA.

Mutations in the gene encoding hepatocyte nuclear factor-4α (HNF-4α) result in maturity-onset diabetes of the young (MODY). To determine the contribution of HNF-4α to the maintenance of glucose homeostasis by the β cell in vivo, we derived a conditional knockout of *HNF-4α* using the Cre-*loxP* system. Surprisingly, deletion of *HNF-4α* in β cells resulted in hyperinsulinemia in fasted and fed mice but paradoxically also in impaired glucose tolerance. Islet perifusion and calcium-imaging studies showed abnormal responses of the mutant β cells to stimulation by glucose and sulfonylureas. These phenotypes can be explained in part by a 60% reduction in expression of the potassium channel subunit Kir6.2. We demonstrate using cotransfection assays that the *Kir6.2* gene is a transcriptional target of HNF-4α. Our data provide genetic evidence that HNF-4α is required in the pancreatic β cell for regulation of the pathway of insulin secretion dependent on the ATP-dependent potassium channel.

Introduction

Maturity-onset diabetes of the young (MODY) is a mendelian form of type 2 diabetes characterized by an autosomal dominant mode of inheritance, early onset, and impaired glucose-stimulated insulin secretion. MODY can result from mutations in at least 6 different genes. One of these encodes the glycolytic enzyme glucokinase (MODY2), which is an important glucose sensor, while all the others encode transcription factors: hepatocyte nuclear factor-4α (*HNF-4α*) (MODY1); *HNF-1α* (MODY3); insulin promoter factor 1 (*IPF1*/pancreatic duodenal homeobox 1 [*Pdx-1*]) (MODY4); *HNF-1β* (MODY5); and neurogenic differentiation factor 1 (*NeuroD1*) (MODY6) (1). Genetic and biochemical studies have revealed that many of these transcription factors participate in a transcriptional regulatory network in both the liver and pancreas.

A hierarchy among MODY genes has been derived from the molecular analysis of MODY, as mutations in both the gene encoding HNF-4α (MODY1) and the binding site for the protein HNF-4α in the *HNF-1α* promoter cause diabetes (2, 3). In addition, more recent studies have demonstrated that mutations in the β cell–specific promoter (P2) of *HNF-4α* in humans are associated with increased risk of type 2 diabetes (4–6). Therefore, it has been proposed that HNF-1α and HNF-4α form a regulatory loop in the adult β cell and that this regulatory loop is essential for β cell function (7, 8). Furthermore, it was hypothesized that haploinsufficiency for either gene can cause a breakdown in the regulatory loop, ultimately resulting in diabetes (9). However, much of the information about the role of HNF-4α in the pancreas so far has been based on expression and biochemical data. For example, when a dominant negative form of HNF-4α was overexpressed in insulinoma cells, several genes involved in glucose metabolism as well as HNF-1α were differentially expressed, suggesting that HNF-4α regulates β cell glucose metabolism through the regulation of *HNF-1α* and several glycolytic and mitochondrial genes (9, 10). Most recently, Odom and colleagues combined chromatin immunoprecipitation with promoter microarrays to identify over 1000 human promoter elements bound by HNF-4α in pancreatic islets, suggesting that HNF-4α may function to regulate multiple pathways in the β cell (11). Although it has been shown that HNF-4α is required for maintenance of the expression of *HNF-1α* and important metabolic genes in the liver, it remains unknown whether this relationship holds true in the pancreatic β cell or whether HNF-4α is essential for β cell glucose metabolism in vivo. Understanding the relationship between MODY genes and their specific functional targets in vivo may identify a common mechanism of pathogenesis and lead to a novel approach for improving β cell function.

MODY1 patients fail to secrete insulin adequately in response to glucose challenge (12). This observation, along with other recent biochemical studies, suggests that HNF-4α plays a role in pancreatic development and/or in the regulation of β cell function. However, the exact role of HNF-4α in the maintenance of β cell function has not to our knowledge been determined in vivo until now. Because targeted disruption of *HNF-4α* in mice results in early death due to defective gastrulation (13, 14), genetic analysis of the function of HNF-4α in the adult pancreas has thus far been precluded. To determine the role of HNF-4α in the β cell and in the maintenance of glucose homeostasis in vivo, as well as its contribution to the molecular etiology of MODY, we have derived a conditional knockout of *HNF-4α* using the Cre-*loxP* system. Deletion of *HNF-4α* in β cells resulted in impaired glucose tolerance but, surprisingly, also in fasting and fed hyperinsulinemia. The data presented here reveal an unpredicted role for HNF-4α in the regulation of the pathway of insulin secretion dependent on the

Nonstandard abbreviations used: BHK, baby hamster kidney; EMSA, electrophoretic mobility-shift assay; Foxa2, forkhead box a2; fura-2AM, fura-2 acetoxymethylester; HNF-4α, hepatocyte nuclear factor–4α; K_{ATP} channel, ATP-dependent potassium channel; MODY, maturity-onset diabetes of the young; NeuroD1, neurogenic differentiation factor 1; Pdx-1, pancreatic duodenal homeobox 1; PP, pancreatic polypeptide.

Conflict of interest: The authors have declared that no conflict of interest exists.

Citation for this article: *J. Clin. Invest.* **115**:1006–1015 (2005). doi:10.1172/JCI200522365.

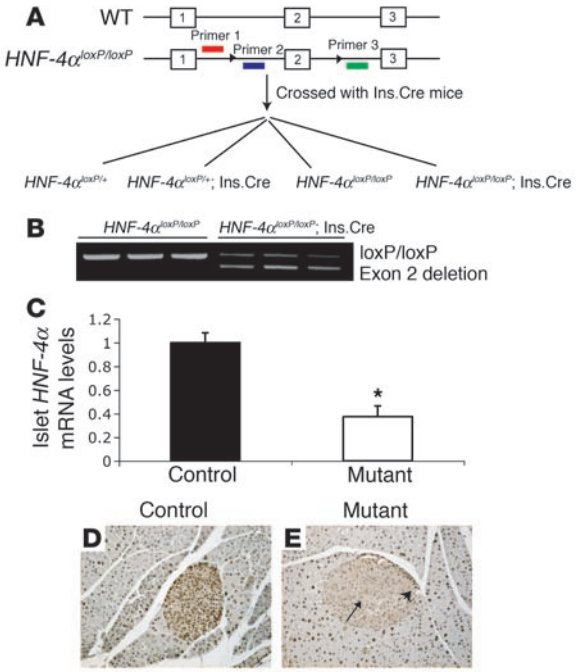

Figure 1
Derivation of β cell–specific *HNF-4α* knockout mice. (**A**) *HNF-4α*$^{loxP/loxP}$ mice in which exon 2 was flanked by *loxP* sites were bred to Ins.Cre-transgenic mice expressing Cre recombinase under control of the rat insulin promoter. The resulting *HNF-4α*$^{loxP/+}$; Ins.Cre offspring were then mated with *HNF 4α*$^{loxP/loxP}$ homozygotes to obtain *HNF-4α*$^{loxP/loxP}$; Ins.Cre mutants and their littermate controls: *HNF-4α*$^{loxP/+}$, *HNF-4α*$^{loxP/loxP}$, and *HNF-4α*$^{loxP/+}$; Ins.Cre. (**B**) Primers 1, 2, and 3 (red, blue, and green in **A**) were used for PCR genotyping of isolated islets from *HNF-4α*$^{loxP/loxP}$; Ins.Cre and *HNF-4α*$^{loxP/loxP}$ mice. In the absence of Cre, amplification by primers 1 and 2 results in a 620-bp product. Cre-mediated excision of exon 2 results in a 450-bp product amplified by primers 1 and 3. Quantification of the bands shows that deletion occurs in approximately 70% of all islet cells (note that non–β cells make up 20–30% of the islet cell numbers). (**C**) Concordant with the results in **B**, mRNA levels of *HNF-4α* were reduced by 63% in mutant islets, as determined by quantitative PCR using primers specific to exon 2. *$P < 0.05$; $n = 3$ per group. (**D** and **E**) Immunostaining of pancreatic sections from adult control (**D**) and mutant (**E**) mice using an antibody against HNF-4α indicates that the number of β cells expressing HNF-4α protein is reduced by approximately 85–90% (arrow) in the mutant mouse. Non–β cells in the islet mantle still express HNF-4α protein (arrowhead) in the mutant mouse. Thus, HNF-4α is deleted efficiently and specifically in pancreatic β cells. Magnification, ×200.

ATP-dependent potassium channel (K_{ATP} channel) and demonstrate that HNF-4α is not required for the maintenance of HNF-1α expression in the adult β cell.

Results

β cell–specific deletion of HNF-4α. In order to obtain mice lacking HNF-4α in pancreatic β cells, we mated *HNF-4α*$^{loxP/loxP}$ mice to mice containing a transgene with Cre recombinase under control of the rat insulin 2 promoter (Ins.Cre) (15). The resulting *HNF-4α*$^{loxP/+}$; Ins.Cre offspring were then bred to *HNF-4α*$^{loxP/loxP}$ homozygotes to obtain *HNF-4α*$^{loxP/loxP}$; Ins.Cre mutants and the littermate groups *HNF-4α*$^{loxP/+}$, *HNF-4α*$^{loxP/loxP}$, and *HNF-4α*$^{loxP/+}$; Ins.Cre (Figure 1A). *HNF-4α*$^{loxP/loxP}$; Ins.Cre mice were born with the expected mendelian distribution and no significant differences in size or appearance were observed at birth or in adult mice (control = 28.6 ± 1.3 grams; mutants = 30.7 ± 1.8 grams; $n = 6$–8 mice; 5 months of age; P = NS) compared with littermate controls (*HNF-4α*$^{loxP/loxP}$ and *HNF-4α*$^{loxP/+}$).

To evaluate the specificity and efficiency of Cre-mediated deletion of HNF-4α, we first used PCR analysis of genomic DNA to determine if the floxed exon 2 of the HNF-4α gene was excised in freshly isolated islets of *HNF-4α*$^{loxP/loxP}$; Ins.Cre and *HNF-4α*$^{loxP/loxP}$ mice (Figure 1B). Primers were designed to amplify a 450-bp product only detectable when the floxed *HNF-4α* gene was deleted. The PCR analysis indicated that gene ablation occurred in approximately 70% of cells in the islets of *HNF-4α*$^{loxP/loxP}$; Ins.Cre mice. Concordantly, mRNA levels of *HNF-4α* in isolated islets of *HNF-4α*$^{loxP/loxP}$; Ins.Cre mice were reduced by approximately 63% compared with those of controls (Figure 1C). Given that 30–40% of islet cells are non–β cells that express HNF-4α, this degree of reduction in whole islets suggests deletion in greater than 90% of β cells. We confirmed the β cell specific inactivation of HNF-4α by examining the expression of HNF-4α protein by immunohistochemistry. HNF-4α is normally found in all cell types of the islet and throughout most of the acinar tissue (Figure 1D). Consistent with previous reports of the use of the Ins.Cre-transgenic line, we found that approximately 90% of pancreatic β cells in the *HNF-4α*$^{loxP/loxP}$; Ins.Cre mice had lost HNF-4α expression by 2–3 weeks after birth, while the expression of HNF-4α was maintained throughout the remainder of the islet as well as in surrounding exocrine tissue (Figure 1E) (15–18). Staining of adjacent sections for insulin and glucagon confirmed the continued presence of HNF-4α protein in α cells, demonstrating the specificity of the Ins.Cre-mediated gene ablation within the pancreas (data not shown).

The Ins.Cre-transgenic mouse used in this study has been reported to excise *loxP* targets ectopically in the central nervous system. This issue is of potential significance, as the hypothalamus plays an important role in glucose homeostasis. However, this ectopic activity of the Ins.Cre transgene is only relevant if the *loxP*-flanked gene to be targeted is expressed in the brain. Multiple expression studies of *HNF-4α* have failed to detect any expression of this gene in the neuroectoderm during development, or in the hypothalamus or other brain regions in the adult mouse, making it extremely unlikely that HNF-4α plays a role in the central nervous system (19, 20). Fasting corticosterone levels, which are controlled by the hypothalamic-pituitary-adrenal axis, in mutant mice are not changed (control, 245 ± 62 ng/ml; mutant, 277 ± 49 ng/ml; $n = 5$ mice; P = NS), supporting the notion that hypothalamic function is maintained in *HNF-4α*$^{loxP/loxP}$; Ins.Cre mice. Thus, it is unlikely that any excision of the floxed *HNF-4α* allele in the brain would contribute to the phenotype of *HNF-4α*$^{loxP/loxP}$; Ins.Cre mice. In addition, our studies on isolated islets described below demonstrate a specific requirement for HNF-4α in the β cell.

β cell deletion of HNF-4α results in hyperinsulinemia and impaired glucose tolerance in vivo. Next we determined the effect of HNF-4α deficiency in the β cell on glucose homeostasis in vivo by measuring fed and fasting blood glucose levels in the *HNF-4α*$^{loxP/loxP}$; Ins.Cre mice. Compared with controls, HNF-4α mutants exhibited a mild decrease in blood glucose levels in both the fed and fasting states (Figure 2A). To determine if this difference in blood

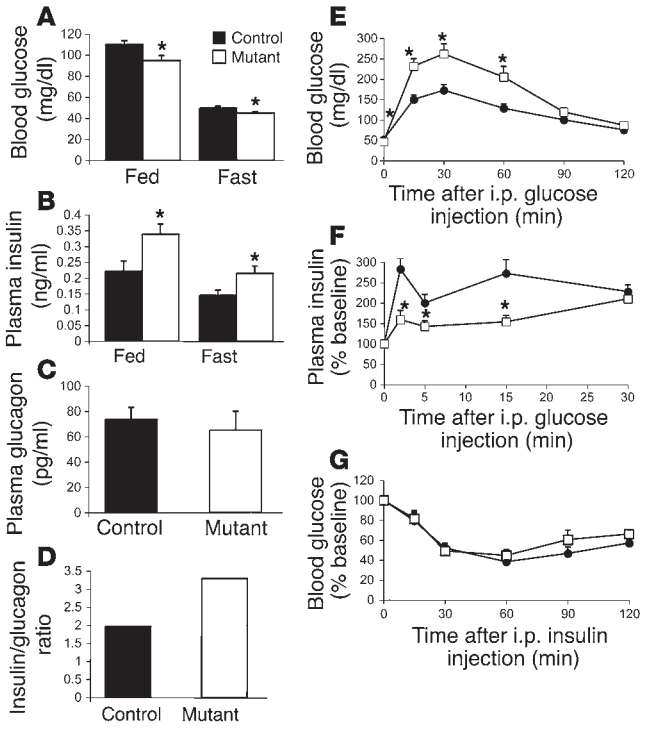

Figure 2
Deletion of HNF-4α in β cells results in hyperinsulinemia and impaired glucose tolerance in vivo. (**A**) In the fed state (Fed) and after an overnight (16-hour) fast (Fast), blood glucose concentrations are decreased in *HNF-4α$^{loxP/loxP}$*; Ins.Cre mice compared with littermate controls. (**B**) Plasma insulin levels are elevated in HNF-4α mutants in both the fed and overnight-fasted states. (**C**) Fasting plasma glucagon levels in the mutants were indistinguishable from controls. (**D**) The ratio of plasma insulin to plasma glucagon is elevated 70% in *HNF-4α$^{loxP/loxP}$*; Ins.Cre mice. (**E**) Glucose tolerance test. After an overnight fast, 3- to 5-month-old *HNF-4α$^{loxP/loxP}$*; Ins.Cre mice and littermate controls were challenged with 2 grams of glucose per kilogram of body weight. The blood glucose elevation is significantly higher in *HNF-4α$^{loxP/loxP}$*; Ins.Cre mice than in controls, indicating impaired glucose tolerance in the HNF-4α mutants. (**F**) Following glucose injection (3 g/kg body weight), HNF-4α mutants exhibit a diminished first-phase insulin secretory response in comparison to controls. (**G**) Insulin tolerance test. Mutant and control mice that had fasted for 4 hours were injected with 0.75 units of insulin per kilogram of body weight. The insulin sensitivity of HNF-4α mutants is indistinguishable from that of controls. **P* < 0.05 by Student's *t* test or ANOVA; *n* = 8–13 animals per group for each experiment.

glucose was a result of changes in circulating levels of insulin and glucagon, we measured plasma levels of these hormones. We found that in both the fed and fasting states, plasma insulin was significantly elevated in the mutants compared with the littermate controls (Figure 2B). In contrast, fasting plasma levels of glucagon were unchanged (Figure 2C). Therefore, the ratio of plasma insulin to plasma glucagon was approximately 70% higher in *HNF-4α$^{loxP/loxP}$*; Ins.Cre mice, which accounted for the lower glucose levels observed in these mice (Figure 2D). Together, these results demonstrate that HNF-4α in the β cell contributes to the maintenance of glucose homeostasis.

Suspecting abnormal regulation of insulin secretion in HNF-4α–deficient β cells, we performed glucose tolerance tests on 3- to 5-month-old HNF-4α$^{loxP/loxP}$; Ins.Cre mice and littermate controls. After glucose injection, the elevation in blood glucose levels was significantly higher in HNF-4α mutants, indicating impaired glucose tolerance in these animals (Figure 2E). As glucose intolerance can result from decreased peripheral insulin sensitivity or impaired glucose stimulated insulin secretion, we measured plasma insulin levels at various time points after glucose challenge. We found that despite a significantly higher basal level of plasma insulin prior to glucose injection (mutant, 0.21 ± 0.02 ng/ml, *n* = 11; control, 0.14 ± 0.02 ng/ml, *n* = 11; *P* < 0.05), plasma insulin levels failed to increase in the mutant mice at the same rate as in controls after injection (Figure 2F). In particular, HNF-4α mutants lacked a robust first-phase insulin secretory response. In order to investigate the possibility that peripheral insulin resistance contributes to the glucose intolerance of HNF-4α mutants, we performed insulin tolerance tests. Both groups of mice showed similar insulin responses (Figure 2G), concordant with the fact that *HNF-4α* is not deleted in the major insulin-responsive tissues in our model. These results indicate that while HNF-4α mutants have higher basal plasma insulin levels, they fail to secrete sufficient insulin in response to exogenous glucose administration and thus suffer from dysregulated insulin secretion and impaired glucose tolerance.

Loss of HNF-4α in the β cell does not affect islet architecture or β cell mass at 4 months of age. Several mechanisms can account for the dysregulation of insulin secretion in vivo, including changes in islet architecture or β cell mass, defective glucose sensing and metabolism, or a combination of these factors. For example, disruption of *HNF-1α* in mice results in defective glucose sensing and the failure of isolated islets from these animals to properly respond to glucose (21, 22). More recent studies have shown that heterozygous deletion of *Pdx-1* in mice results in a decrease in β cell mass due to an increase in islet apoptosis (23).

To determine the effect of HNF-4α deficiency in the β cell on islet architecture, we performed indirect immunofluorescence using antibodies raised against the pancreatic hormones insulin, glucagon, somatostatin, and pancreatic polypeptide (PP) to label 4 major islet cells types: β cells, α cells, δ cells, and PP cells, respectively. We found that both the control mice (Figure 3, A and C) and *HNF-4α$^{loxP/loxP}$*; Ins.Cre mice (Figure 3, B and D) contained all 4 pancreatic islet cell types, with the insulin-producing β cells centrally located within the islet and the less-frequent α cells, δ cells, and PP cells (not shown) located on the periphery. In addition, using point-counting morphometry, we determined the β cell mass in both *HNF-4α$^{loxP/loxP}$*; Ins.Cre mice and littermate controls at 4 months of age and found no significant difference between the 2 groups (control, 0.93 ± 0.17 mg, *n* = 6; mutant, 1.04 ± 0.22 mg, *n* = 5; *P* = NS) (Figure 3E). Together, these results indicate that HNF-4α is not required in the β cell for the maintenance of islet architecture or β cell mass at this age, suggesting that the defect in insulin secretion is a consequence of loss of β cell function rather than β cell differentiation.

Diminished first-phase insulin secretion from isolated islets of HNF-4α mutant mice. We performed insulin secretion studies of perifused

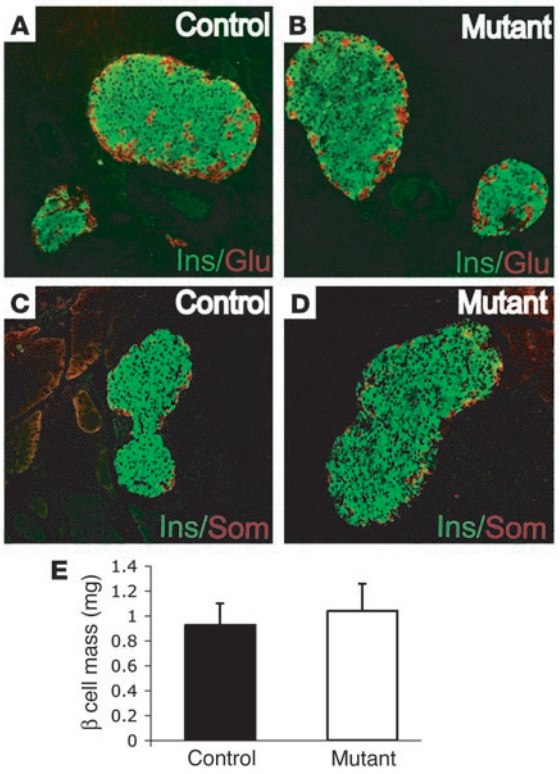

Figure 3
HNF-4α is not required for the maintenance of islet architecture or β cell mass. (**A**–**D**) Immunofluorescence detection of the pancreatic hormones insulin, glucagon, and somatostatin, which label β cells, α cells, and δ cells, respectively. Similar to controls (**A** and **C**), 3- to 5-month-old *HNF-4α*$^{loxP/loxP}$; Ins.Cre mice contain glucagon-positive α cells (**B**) and somatostatin-positive δ cells (**D**). In addition, insulin-positive β cells are centrally located in the islets of both controls and mutants, while less-frequent α cells and δ cells are found along the periphery (**A**–**D**), indicating normal islet architecture in the *HNF-4α*$^{loxP/loxP}$; Ins.Cre mice. Magnification, ×200. (**E**) Point-counting morphometry of 4-month-old mice reveals no significant difference in β cell mass between controls and mutants (control, 0.93 ± 0.17 mg, $n = 6$; mutant = 1.04 ± 0.22 mg, $n = 5$; P = NS).

islets to define the mechanistic defect in *HNF-4α*$^{loxP/loxP}$; Ins.Cre mice. We treated islets with 0–30 mM glucose, which elicited a robust insulin secretory response in control islets (Figure 4A). In contrast, mutant islets lacked a first-phase secretory response to glucose. In addition, mutant islets failed to terminate insulin secretion when reexposed to buffer containing 0 mM glucose. Depolarization with KCl at the end of each experiment confirmed that the islets had remained viable throughout the experiment.

HNF-4α–deficient β cells exhibit a diminished response to glyburide. Glucose-stimulated insulin secretion from the pancreatic β cell occurs after the generation of ATP from the metabolism of glucose through glycolysis and the Krebs cycle. The intracellular rise in the ATP/ADP ratio leads to the closure of the K_{ATP} channels, calcium influx, and subsequent activation of insulin secretion through calcium-dependent pathways (24). This K_{ATP}-dependent pathway is the best characterized mechanism leading to insulin secretion and is essential for proper first-phase insulin release.

We investigated whether components of this pathway were disrupted in *HNF-4α*$^{loxP/loxP}$; Ins.Cre mice by first measuring ATP levels in isolated islets stimulated with various concentrations of glucose. We found that at physiological glucose concentrations (2, 5, and 10 mM), ATP levels in HNF-4α deficient β cells were indistinguishable from those of controls (Figure 4B), suggesting that glucose metabolism is maintained in mutant β cells. To determine if calcium influx occurs properly in response to glucose, we performed calcium-imaging experiments using cultured isolated islets. In response to 16.7 mM glucose, intracellular calcium increased rapidly in control β cells and then diminished when the addition of exogenous glucose was stopped (Figure 4C). However, intracellular calcium increased at a slower rate in mutant islets and failed to decrease as rapidly when glucose was stopped (Figure 4D). To determine if other insulin secretagogues can trigger proper calcium influx, we treated islets with the K_{ATP} channel blocker glyburide as well as with KCl to fully depolarize the plasma membrane. In control islets, glyburide and KCl treatment resulted in a strong and rapid rise in intracellular calcium (Figure 4C). In contrast, intracellular calcium increased at a slower rate in mutant islets exposed to glyburide, but increased normally in response to KCl (Figure 4D).

HNF-4α is required for potassium channel subunit Kir6.2 expression in the pancreatic β cells. The observation that both KCl-induced calcium influx and insulin release as well as glucose metabolism in mutant mice are indistinguishable from those of controls suggested a defect downstream of glucose metabolism but upstream of the voltage-gated calcium channels. The diminished response to glyburide pointed to a defect in K_{ATP}-channel function. Therefore, we examined mRNA levels of the 2 essential subunits of the channel, SUR1 and Kir6.2. While no statistically significant differences were observed in SUR1 subunit expression, mRNA and protein levels of Kir6.2 were downregulated by 40% and 60%, respectively, in the islets of *HNF-4α*$^{loxP/loxP}$; Ins.Cre mice (Figure 5, D and F). Given that Kir6.2 and SUR1 are expressed in α cells as well as β cells and that the Ins.Cre transgene mediates *HNF-4α* deletion only in approximately 85% of β cells, the actual reduction in Kir6.2 expression in HNF-4α–deficient β cells is likely to be greater than 60%. This reduced expression of Kir6.2 provides a possible molecular link between the loss of HNF-4α in the β cell and the dysregulation of insulin secretion observed in vivo and in vitro in *HNF-4α*$^{loxP/loxP}$; Ins.Cre mice (see Discussion).

Prior studies using forced overexpression of either wild-type or a dominant negative version of HNF-4α in insulinoma cells had suggested a range of HNF-4α targets, many of them involved in glycolysis or mitochondrial function (10). Of these genes, only the gene encoding L-pyruvate kinase was differentially expressed in isolated islets of HNF-4α mutant mice (Figure 5C). Other important metabolic genes such as those encoding GLUT2, glucokinase, aldolase B, oxoglutarate dehydrogenase, and insulin, previously identified as putative HNF-4α targets, were not differentially expressed. The maintenance of normal expression of these genes is consistent with the unchanged ATP production in response to glucose in *HNF-4α*$^{loxP/loxP}$; Ins.Cre mice described above (Figure 4B).

Previous studies have suggested that HNF-4α may exert its function in the pancreatic β cell through the regulation of HNF-1α expression (9, 10) and that the regulation of HNF-1α by HNF-4α is a component of a transcriptional regulatory loop that exists in the adult β cell (11). However, using quantitative real-time PCR and Western blot analysis, we found that HNF-4α is not required for the maintenance of HNF-1α mRNA or protein expression in the adult β cell (Figure 5, A and E). In addi-

tion, we did not find significant differences in mRNA levels of other MODY genes, including *HNF-1*β, *Pdx-1*, and *NeuroD1*, or those encoding other pancreatic transcription factors that regulate insulin secretion (Figure 5, A and B). Levels of mRNA in the gene encoding Foxa2, an essential regulator of Kir6.2 expression, were not altered significantly (18, 25). However, expression of the nuclear receptor HNF-4γ was significantly reduced by approximately 34%, indicating that HNF-4α is required for normal expression of its related family member. Furthermore, PPARα, a target of HNF-4α in the liver (26) postulated to play a role in the β-oxidation of lipids in β cells (27), was downregulated by approximately 70% in mutant islets (Figure 5B).

HNF-4α binds the Kir6.2 promoter and activates the Kir6.2 gene in cotransfection assays. To evaluate whether HNF-4α can directly regulate Kir6.2 expression at the transcriptional level, we searched for potential HNF-4α binding sites in the *Kir6.2* promoter. A putative HNF-4α binding site was identified 2,300 bp upstream of the transcriptional start site (Figure 6, A and B). In order to determine if HNF-4α can bind this sequence of the *Kir6.2* promoter, we performed electrophoretic mobility shift assays (EMSAs). Incubation of wild-type liver nuclear extract with a radiolabeled oligonucleotide containing the putative HNF-4α binding site sequence resulted in a strong shift of the radioactive band (Figure 6C). The addition of an antibody against HNF-4α generated a supershifted band comparable to that achieved with the consensus site probe, but was not observed with preimmune serum, indicating that the bound protein was indeed HNF-4α. These results were also confirmed using an additional antibody against HNF-4α. To determine if the cis-regulatory element in the *Kir6.2* gene can function as an HNF-4α–dependent enhancer, we performed cotransfection assays with a 237-bp region of the *Kir6.2* gene containing the HNF-4α binding site cloned into a luciferase promoter plasmid and an HNF-4α expression vector. We found that overexpression of HNF-4α in baby hamster kidney (BHK) cells resulted in an increase of approximately 5-fold in luciferase activity and that this transcriptional activation was abolished when the HNF-4α binding site sequence was mutated (Figure 6D). Our results demonstrate that HNF-4α is a transcriptional activator of the *Kir6.2* gene.

Discussion

MODY is a monogenic form of diabetes characterized by early onset and the progressive loss of insulin secretory capacity (28). Several recent reports have suggested that the MODY1 subtype results from the loss of HNF-4α function in the pancreas and that HNF-4α functions as "master regulator" of multiple transcriptional networks in the islet (11). However, the specific role for HNF-4α in the maintenance of β cell function has not to our knowledge been established until now. Here we have attempted to address this question by genetic means.

We used the Cre-*loxP* recombination system to delete *HNF-4α* in β cells of the adult pancreas. We found that 3- to 5-month-old *HNF-4α*$^{loxP/loxP}$; Ins.Cre mice exhibited elevated plasma insulin levels in the fasted and fed states but also suffered from impaired glucose tolerance. Although these results provide evidence that HNF-4α is required in the β cell for the regulation of insulin secretion, the overall phenotype of these animals was quite surprising, considering the hypoinsulinemic hyperglycemia present in humans with reduced HNF-4α function. Given the relatively late onset of MODY1 in humans (15–25 years) compared with the age of our mice (3–5 months), and given that in MODY1 patients, HNF-4α function is impaired in the liver in addition to β cells, it appears likely that long-term and cumulative damage to the β cell contributes to the more severe phenotype observed in humans. However, consistent with the observations made in MODY1 patients, *HNF-4α*$^{loxP/loxP}$; Ins.Cre mice failed to secrete adequate amounts of insulin after glucose stimulation and thus are glucose intolerant. This can be explained by our finding that isolated islets lacking HNF-4α demonstrated an abnormal response to glucose in perifusion experiments, including an attenuated first phase of insulin secretion.

Also surprising is the finding that HNF-1α, which is dependent on HNF-4α in hepatocytes (26), was not differentially expressed

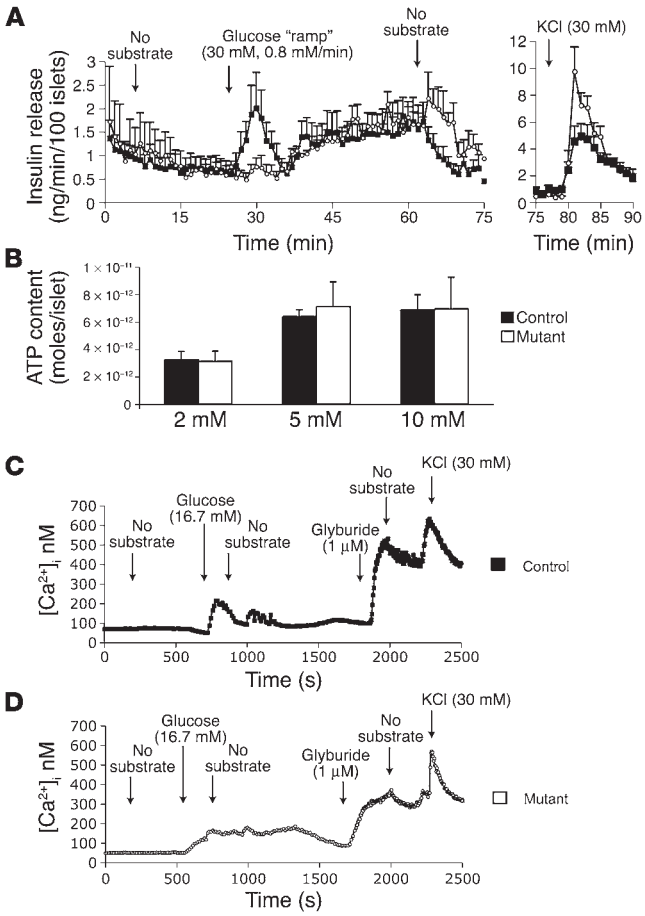

Figure 4

Glucose-stimulated insulin secretion is dysregulated in isolated islets of *HNF-4α*$^{loxP/loxP}$; Ins.Cre mice. (**A**) Isolated islets from HNF-4α mutants (open circles) lack a robust first-phase insulin secretory response to glucose perifusion compared with that of controls (filled squares), and fail to rapidly terminate insulin secretion upon switching to 0 mM glucose (n = 3). (**B**) ATP levels in isolated islets from *HNF-4α*$^{loxP/loxP}$; Ins.Cre mice (white bars) stimulated with 2, 5, or 10 mM glucose for 60 minutes are virtually indistinguishable from those of control mice (black bars) (n = 2 per group), indicating that glucose metabolism is not adversely affected in HNF-4α–deficient β cells. (**C**) The intracellular calcium concentration ($[Ca^{2+}]_i$) increases rapidly in response to 16.7 mM glucose (2.9 nM/s), 1 μM glyburide (10.0 nM/s), and 30 mM KCl in control islets. (**D**) In contrast, the intracellular calcium concentration increases at a slower rate in response to glucose (0.7 nM/s) and glyburide (2.0 nM/s) in *HNF-4α*$^{loxP/loxP}$; Ins.Cre mice. For all calcium-imaging experiments, n = 4 per group. These are representative plots.

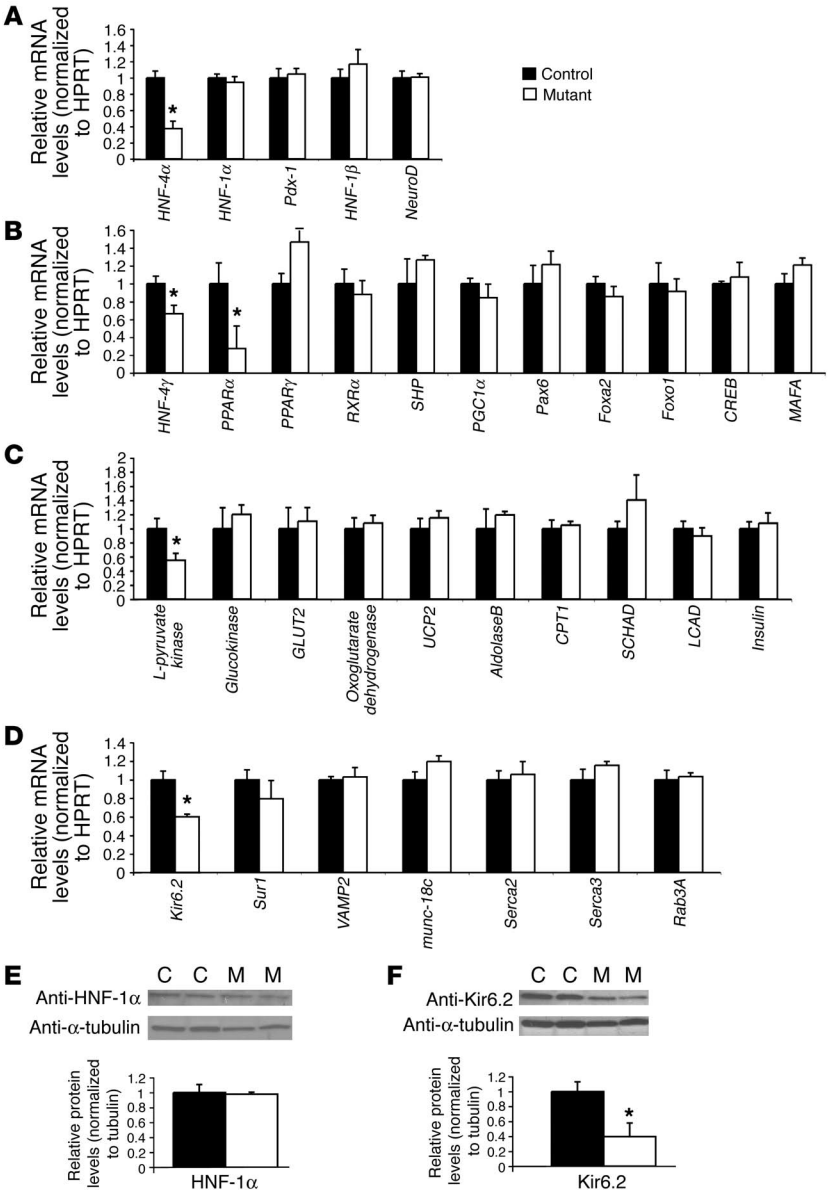

Figure 5
Gene expression analysis in isolated islets of *HNF-4α$^{loxP/loxP}$*; Ins.Cre mice. (**A**) Levels of mRNA of MODY genes, as determined by real-time PCR. (**B**) Levels of mRNA of pancreatic enriched transcription factors, as determined by real-time PCR. (**C**) Levels of mRNA of genes involved in glucose and lipid metabolism, as determined by real-time PCR. (**D**) Levels of mRNA of genes involved in stimulus-secretion coupling, as determined by real-time PCR. *$P < 0.05$; $n = 3$–5 for all PCR experiments. HPRT, hypoxanthine guanine phosphoribosyl transferase. (**E**) Western blot analysis of HNF-1α in isolated islets normalized to α-tubulin protein levels. C, control; M, mutant. (**F**) Western blot analysis of Kir6.2 in isolated islets normalized to α-tubulin protein levels. For all protein quantification, $n = 3$, controls, and $n = 2$, mutants.

at the mRNA or protein level in HNF-4α mutant islets. Given the reports that HNF-4α binds to the *HNF-1α* promoter and that a mutation in the HNF-4α binding site on the *HNF-1α* promoter leads to MODY, one would expect HNF-4α to be an essential regulator of HNF-1α expression in the β cell (3, 11). However, as described by Servitja and colleagues, it is likely that the regulatory relationships between MODY genes vary between tissues and developmental stages (8). Although our results demonstrate that HNF-4α is not required for the *maintenance* of HNF-1α expression in adult β cells, it remains possible that HNF-4α is required for the *initiation* of HNF-1α expression earlier during pancreatic development. Another possibility is that the regulatory relationship is more important in the liver than in the β cell. However, the downregulation of HNF-4γ and PPARα suggests that HNF-4α functions in a transcriptional regulatory network involving other nuclear receptors.

Given the report by Wang and colleagues that HNF-4α regulates the expression of genes associated with β cell glucose metabolism and insulin secretion in insulinoma cells (10), we initially hypothesized that altered expression of these genes and a defect in glucose metabolism in HNF-4α–deficient β cells may relate to the observed phenotype of these mice. However, of all of the targets suggested to be dependent upon HNF-4α in that study, only L-pyruvate kinase was significantly reduced in the islets of *HNF-4α$^{loxP/loxP}$*; Ins.Cre mice. This discrepancy may be explained by the fact that Wang and colleagues used insulinoma cells and overexpressed HNF-4α to levels at which the protein will bind promoters that it will not normally bind in vivo. It is also likely that several redundant transcriptional regulatory mechanisms exist in the adult β cell. Odom and colleagues identified several cases of "multiple input regulatory circuits" in the β cell that are controlled by a number of transcription factors (11). Given the overlap of target promoters bound by HNF-1α, HNF-4α, and other pancreatic transcription factors, it is possible that these other proteins can compensate for the loss of HNF-4α to maintain gene expression. Interestingly, analogous overexpression studies with a dominant negative HNF-1α in the same insulinoma cell line resulted in a similar phenotype and gene expression profile, as was the case with the dominant negative HNF-4α (29). However, when Shih and colleagues performed a comprehensive gene expression analysis of HNF-1α–deficient islets, they found discrepancies with the insulinoma studies similar to those we have reported here (22). Furthermore, it has been shown that downregulation of L-pyruvate kinase in pancreatic islets has little effect on overall pyruvate kinase activity, consistent with the finding that the M_2-pyruvate kinase isoform predominates in β cells (30, 31). Thus, it is unlikely that changes in L-pyruvate kinase expression explain the observed phenotype of *HNF-4α$^{loxP/loxP}$*; Ins.Cre mice. In addition, our results, as well as the results reported by Shih and colleagues, further emphasize the need for animal models with which to study the functional requirements of transcription factors in the regulation of β cell gene expression.

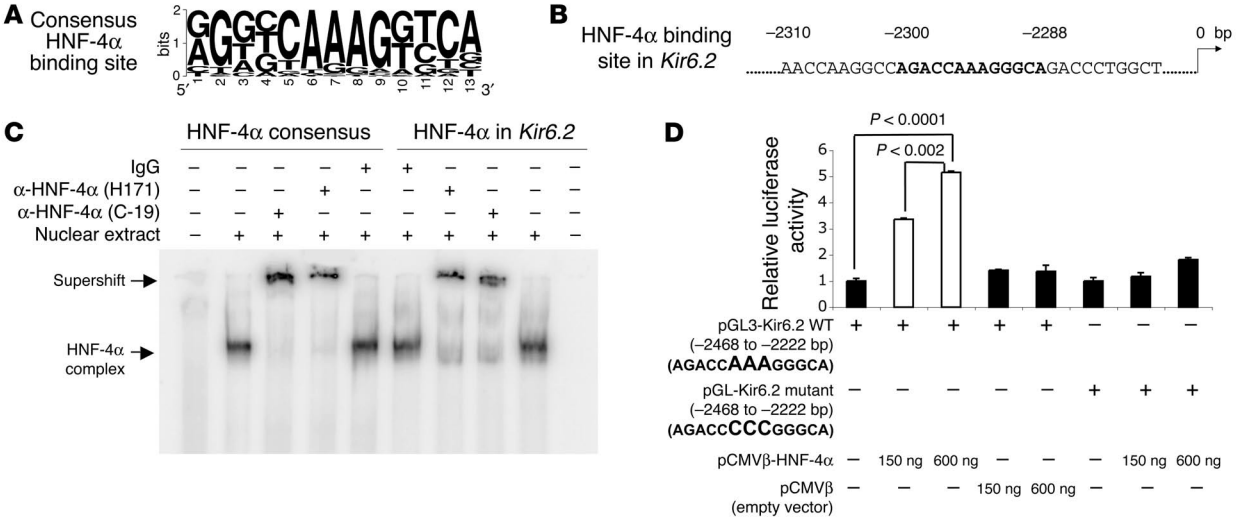

Figure 6

HNF-4α directly activates the *Kir6.2* gene. (**A**) The consensus binding site for HNF-4α is 13 bp long and was derived from 71 known HNF-4α binding sequences from the literature (55) using the program Weblogo (http://weblogo.berkeley.edu/). The size of the letters reflects the frequency at which the nucleotide appears at that position in the binding site. (**B**) Putative HNF-4α binding site in the Kir6.2 promoter identified using NUBIScan, which uses a transcription factor–binding site–identification algorithm to identify nuclear receptor binding sites. Note that the site located at position –2,300 matches all determinant nucleotides in the HNF-4α consensus site shown in **A**. (**C**) EMSA demonstrates that HNF-4α binds to the identified binding site in the *Kir6.2* gene as well as the HNF-4α consensus site. In supershift experiments using 2 different antibodies raised against HNF-4α, the identity of the bound protein is confirmed to be HNF-4α. (**D**) Cotransfection of BHK cells with HNF-4α and pGL3-Kir6.2, expressing luciferase under the control of the 237-bp region of *Kir6.2* containing the binding site, results in a dose-dependent increase in luciferase activity, indicating that this element serves as an HNF-4α–dependent enhancer. Mutation of this binding site abolishes the transcriptional activation. Statistical analysis was performed by ANOVA; $n = 3$ for each transfection condition.

Using the *HNF-4α*$^{loxP/loxP}$; Ins.Cre mouse model, we have revealed an unexpected role for HNF-4α in the regulation of the K_{ATP} channel–dependent pathway of glucose-stimulated insulin secretion. We have found that HNF-4α is required in the β cell for the maintenance of normal Kir6.2 mRNA and protein expression and that HNF-4α is a transcriptional activator of the *Kir6.2* gene. Because Odom and colleagues examined only promoter elements located –700 bp to +200 bp relative to the transcriptional start site in their location analysis (11), they failed to identify target genes that are bound by HNF-4α further upstream, such as *Kir6.2*. The importance of Kir6.2 function in glucose homeostasis has been clearly established, because mutations in the *Kir6.2* locus in humans can lead to persistent hyperinsulinemic hypoglycemia of infancy (32, 33). In addition, several mouse models have demonstrated the importance of the K_{ATP} channel in maintaining β cell function (34–38). In particular, expression of a dominant negative form of Kir6.2 or targeted disruption of the Kir6.2 gene in mouse β cells leads to a reduction in or loss of K_{ATP} channel function and, consequently, elevated basal calcium levels and impaired glucose-stimulated insulin secretion from isolated islets (34, 36, 37). More recently, Li and colleagues used a hammerhead ribozyme to reduce *Kir6.2* mRNA levels in RINm5F cells, resulting in a 60% decrease in K_{ATP} channel density, sufficient to diminish glucose-stimulated insulin release (35). In addition to the observed defects in glucose and sulfonylurea induced insulin secretion, another hallmark of K_{ATP} channel–deficient mice is the inability of isolated islets to properly shut off calcium influx and insulin secretion upon glucose withdrawal (39). The insulin secretory defects and calcium responses we have described here for *HNF-4α*$^{loxP/loxP}$; Ins.Cre mice resemble many of the defects in K_{ATP} channel–deficient mice. It should be noted that because Kir6.2 levels are reduced but not absent in the HNF-4α mutants, the β cell defect in *Kir6.2*$^{-/-}$ mice is more severe than the defect in HNF-4α–deficient β cells. Nevertheless, *Kir6.2*$^{-/-}$ mice paradoxically exhibit an even more mild impairment in glucose tolerance. This is explained by the finding that *Kir6.2*$^{-/-}$ mice are *hypersensitive* to insulin due to the critical role of Kir6.2 in regulating glucose uptake by adipose tissue and skeletal muscle (36, 40). In *HNF-4α*$^{loxP/loxP}$; Ins.Cre mice that we have derived here the expression of HNF-4α is lost only in the pancreatic β cells of the islet. Therefore, the skeletal muscle defects seen in *Kir6.2*$^{-/-}$ mice are not be present in the HNF-4α mutants. This was confirmed by the normal insulin sensitivity of *HNF-4α*$^{loxP/loxP}$; Ins.Cre mice (Figure 2G). However, transgenic mouse models of Kir6.2 have been reported in which a dominant negative form of Kir6.2 is expressed specifically in β cells (34, 37). Similar to *HNF-4α*$^{loxP/loxP}$; Ins.Cre mice, Kir6.2-transgenic mice are hyperinsulinemic and exhibit defects in glucose-stimulated insulin secretion from isolated islets, including the loss of the first phase of insulin secretion, and abnormal calcium influx in response to glucose and sulfonylureas (34). Therefore, we propose that the maintenance of Kir6.2 expression by HNF-4α is necessary for normal glucose-stimulated insulin secretion and that the downregulation of Kir6.2 contributes in part to the observed phenotype of the HNF-4α mutant mice.

Although our data have shown that HNF-4α is required in the adult β cell for the regulation of insulin secretion, the absence of HNF 4α from the β cells of 5-month-old *HNF-4α*$^{loxP/loxP}$; Ins.Cre mice is not sufficient to trigger the onset of overt diabetes. Several possibilities may explain this observation. First, the loss of HNF-4α from β cells of *HNF-4α*$^{loxP/loxP}$; Ins.Cre mice may lead to hypergly-

cemia with increased age, in the presence of genetic modifiers, or in the presence of environmental factors such as a high-fat diet. The same factors have been shown to play a role in the eventual development of hyperglycemia observed in older Kir6.2-deficient mice. Older mice transgenic for a dominant negative mutant of Kir6.2 develop hyperglycemia and glucose intolerance (37). The progression to hyperglycemia is accelerated when these mice are fed a high-fat diet (41). Second, several mechanisms for nutrient-stimulated insulin secretion exist in the β cell. The mild impairment in glucose tolerance exhibited by K_{ATP} channel–deficient mice has been explained in part by the increased activity of K_{ATP} channel–independent pathways leading to insulin secretion (42, 43). Thus, while HNF-4α is essential for K_{ATP} channel–dependent insulin secretion, it is possible that other pathways that potentiate nutrient-stimulated insulin secretion can compensate in the short term to prevent more-severe impairments in glucose homeostasis. One possible alternate pathway is suggested by our finding that expression of the nuclear receptor PPARα was reduced in HNF-4α–deficient β cells. PPARα has been shown to activate genes encoding enzymes of the β-oxidation pathway of fatty acids. A decrease in β-oxidation is suggested to result in the accumulation of lipids in the cytoplasm, resulting ultimately in increased insulin secretion (44, 45). Given the postulated role of PPARα in the regulation of β cell lipid metabolism, it is possible that the lower level of PPARα in the HNF-4α mutants partially contributes to the elevated basal insulin levels (27). Third, as described above, it is possible that HNF-4α also plays an important role in the developing pancreas prior to excision of the floxed *HNF-4α* allele by the Ins.Cre transgene. Like many other pancreatic transcription factors such as Pdx-1 (MODY4) or Foxa2, HNF-4α may be required at multiple stages of pancreatic development. Finally, it is also likely that in mice and humans, contributions of other HNF-4α–deficient organs are necessary for the progression to type 2 diabetes. MODY 1 diabetics exhibit impairments in lipid homeostasis prior to the onset of hyperglycemia, indicating a primary hepatic lesion in these patients (46). Targeted disruption of HNF-4α in the adult liver also results in impaired lipid homeostasis, abnormal glycogen deposition, and hepatic hypertrophy (26). More recently, Parviz and colleagues have demonstrated the importance of HNF-4α in the formation of a hepatic epithelium during liver development (47). Thus, this raises the possibility that haploinsufficiency for *HNF-4α* in the liver also contributes to the progression of hyperglycemia in MODY1. Supporting this hypothesis are studies of MODY5. Patients with mutations in the MODY5 gene *HNF-1β* suffer diabetes and renal dysfunction (48). However, mice with a targeted deletion of *HNF-1β* in β cells are glucose intolerant due to impaired insulin secretion but do not exhibit hyperglycemia, providing another example of how the loss of a MODY gene only in the β cell may not be sufficient to trigger overt diabetes (49). Nevertheless, the model of HNF-1β and the model of HNF-4α reported in this article provide excellent tools to elucidate the mechanisms by which these MODY genes contribute to the maintenance of glucose homeostasis by the β cell.

In summary, our data provide genetic evidence that HNF-4α is required in the adult β cell for the regulation of β cell function. Our data also reveal an unexpected role for HNF-4α in the regulation of the K_{ATP} channel–dependent pathway of insulin secretion. The model derived here will serve as a useful tool for identifying additional genes and pathways dependent on HNF-4α activity and may lead to novel treatment regimens for type 2 diabetes.

Methods

Animals and genotype analysis. The derivation of both *HNF-4α*$^{loxP/loxP}$ and Ins.Cre mice has been reported previously (15, 50). All mice were maintained on the CD1 background. Genotyping was performed by PCR analysis using genomic DNA isolated from the tail tips of newborn mice. All of the experiments described here focused on female mice, because female *HNF-4α*$^{loxP/loxP}$;Ins.Cre mice showed larger impairments in glucose homeostasis compared with age- and sex-matched control mice on a standard diet than did male mice (Figure 2). Littermate *HNF-4α*$^{loxP/loxP}$ and *HNF-4α*$^{loxP/+}$ female mice were used as controls. All procedures involving mice were approved by the University of Pennsylvania Institutional Animal Care and Use Committee.

Immunofluorescence and immunohistochemistry. Indirect immunofluorescence was performed as described previously (18) and was examined using confocal microscopy (Leica Microsystems Inc.). The following antibodies were used: guinea pig anti-insulin (1:800 dilution; Linco Research Inc.), rabbit anti-glucagon (undiluted; Zymed Laboratories Inc.), rabbit anti-somatostatin (1:50 dilution; Zymed Laboratories Inc.), indocarbocyanine-conjugated donkey anti-rabbit IgG (1:750 dilution; Jackson ImmunoResearch Laboratories Inc.), and carbocyanine-conjugated donkey anti–guinea pig IgG (1:200 dilution; Jackson ImmunoResearch Laboratories Inc.).

For immunohistochemistry, slides were blocked with avidin D and biotin blocking reagents (Vector Laboratories) for 15 minutes at room temperature with a quick rinse in PBS in between. All slides were blocked with protein-blocking reagent (Immunotech) for 20 minutes at room temperature. Anti–HNF-4α (SC-6556; Santa Cruz Biotechnology) was diluted in phosphate buffered saline plus tween (PBT) and was incubated with tissue overnight at 4°C. Slides were washed in PBS and were incubated with biotinylated anti-goat. HRP-conjugated avidin–biotinylated enzyme complex reagent was used following the manufacturer's protocol (Vector Laboratories). Signals were developed using 3,3-diaminobenzidine tetrahydrochloride as substrate. For β cell mass determination, pancreata were laid flat during the paraffin-embedding process. The section with the largest tissue surface area was stained for insulin by immunohistochemistry as outlined above. Quantification of β cell mass was performed as described previously (16).

Glucose and insulin tolerance tests. For glucose tolerance tests, animals that had fasted overnight (16 hours) were injected intraperitoneally with 2 grams of glucose (Sigma-Aldrich) per kilogram of body weight. Glucose levels were measured at 0, 15, 30, 60, 90, and 120 minutes with Glucometer Elite (Bayer Corporation). For determination of plasma insulin concentrations during glucose tolerance tests, animals that had fasted overnight were injected with 3 grams of glucose per kilogram of body weight and blood was collected from the tail vein at 0, 2, 5, 15, and 30 minutes after injection. Plasma insulin measurements were performed by ELISA (Crystal Chem Inc.) For insulin tolerance tests, mice that had fasted for 4 hours were injected intraperitoneally with 0.75 units of insulin per kilogram of body weight. Glucose levels were measured at 0, 15, 30, 60, 90, and 120 minutes as described above.

Islet perifusions. For each experiment, 100 islets were isolated from 3- to 5-month-old mutants and controls using standard collagenase digestion followed by purification through a Ficoll gradient (51). One hundred islets were "hand-picked" under a light microscope and were placed into a perifusion chamber (Millipore). A computer-controlled fast-performance HPLC system (625 LC System; Waters Corporation) allowed for programmable rates of flow and concentration of the appropriate solutions held at 37°C in a water bath. Islets were perifused with Krebs bicarbonate buffer (2.2 mM Ca^{2+}, 0.25% bovine serum albumin, 10 mM HEPES [acid], and 95% O_2 and 5% CO_2 equilibration, pH 7.4) to reach baseline hormone secretion values before the addition of the appropriate secretagogues. Samples were

collected at regular intervals with a fraction collector (Waters Corporation) and insulin content was determined using a radioimmune assay (University of Pennsylvania Diabetes Center).

ATP assays. Isolated islets were cultured at 37°C and 5% CO_2 for 3 days in RPMI 1640 medium (glucose-free; Sigma-Aldrich) supplemented with 10% FBS, 2 mM glutamine, 100 units/ml penicillin, 50 μg/ml streptomycin, and 10 mM glucose. Then, 50 islets per condition were preincubated for 90 minutes at 37°C and 5% CO_2 in glucose-free Krebs bicarbonate buffer and then were incubated for 60 minutes in buffer containing the indicated amounts of glucose (Figure 4B). ATP was extracted from islets and assayed as described previously (52).

Calcium-imaging. Isolated islets were cultured for 3 days in 10 mM glucose and were pretreated at 37°C for 40 minutes in Krebs bicarbonate buffer supplemented with 1 mM fura-2 acetoxymethylester (fura-2AM; Invitrogen Corp.). The fura-2AM–loaded islets were transferred to a perifusion chamber and were placed on the homeothermic platform of an inverted Zeiss microscope for visualization with a 40× oil-immersion objective (Carl Zeiss MicroImaging Inc.). Islets were perifused with Krebs bicarbonate buffer at 37°C at a flow rate of 2 ml/min while various treatments were applied. The intracellular calcium concentration was determined by the ratio of the excitation of fura-2AM at 334 nm to that at 380 nm. Emission was measured at 520 nm with an Attofluor charge-coupled device camera and was calibrated using Attofluor Ratio Vision Software (BD Biosciences). The rate of change in intracellular calcium was calculated from the first 6 data points starting with the data point prior to the first observed increase in calcium.

Real-time PCR and Western blot analysis. Islets from 3- to 5-month-old mice were isolated using the standard collagenase procedure as described above. Total RNA from islets was isolated in Trizol (Invitrogen Corp.) according to the manufacturer's instructions. Islet RNA was reverse-transcribed using 1 μg oligo(dT) primer, Superscript II Reverse Transcriptase, and accompanying reagents (Invitrogen Corp.). PCR reaction mixes were assembled using the Brilliant SYBR Green QPCR Master Mix (Stratagene). Reactions were performed using the SYBR Green (with Dissociation Curve) program on the Mx4000 Multiplex Quantitative PCR System (Stratagene). All reactions were performed in triplicate with reference dye normalization, and median cycling threshold values were used for analysis. Primer sequences are available upon request. Islet purity was assessed as previous described (25). For Western blots, islet extracts were prepared as described previously (53), were separated by SDS-PAGE, were transferred to immobilin P membranes (Millipore), and were probed with rabbit polyclonal anti-Kir6.2 (Chemicon International Inc.), rabbit anti–HNF-1α (Santa Cruz Biotechnology Inc.), and monoclonal anti–α-tubulin (Sigma-Aldrich). The ECL Plus detection system was used to detect the signal (Amersham Pharmacia). Band intensities were quantified using the QuantityOne 4.3.1 program (Biorad Laboratories). Intensities were normalized to those obtained for α-tubulin.

Computational identification of HNF-4α binding sites in the Kir6.2 promoter. For the identification of potential HNF-4α binding sites in the *Kir6.2* promoter, 4.5 kilobases of promoter sequence upstream of the transcriptional start site was retrieved from the University of California Santa Cruz Genome Browser (http://www.genome.ucsc.edu) and was uploaded into the NUBIScan website (http://www.nubiscan.unibas.ch), which uses an *in silico* approach for predicting nuclear receptor response elements (54). A directed search for DR1 (direct repeat with single nucleotide spacing) half-sites using the HNF-4α matrix was performed to identify the putative binding sites. The site with the highest score was analyzed in gel-shift and cotransfection experiments.

EMSA. Oligonucleotides were synthesized corresponding to the HNF-4α consensus site (sc-2599; Santa Cruz Biotechnology Inc.) and to the HNF-4α inding site in the *Kir6.2* gene located 2.3 kilobases upstream of the transcriptional start site. Radiolabeled probes were generated by the incubation of 250 ng of annealed oligonucleotides for 15 minutes at 37°C with 20 μCi [^{32}P]dCTP in the presence of Klenow DNA polymerase (Roche Applied Science). Radiolabeled probes were subsequently separated from free nucleotide using G-50 column purification (Amersham Biosciences). Liver nuclear extract (a kind gift from L.E. Greenbaum, University of Pennsylvania, Philadelphia, Pennsylvania, USA) was then incubated at room temperature for 15 minutes with radiolabeled probe at 100,000 dpm and 1 μg poly(dI-dC) in 10 mM Tris-HCl, pH 7.5, 50 mM NaCl, 1 mM DTT, 1 mM EDTA, and 5% glycerol. Binding reactions were then incubated with the specified Santa Cruz HNF-4α antisera for 30 minutes at room temperature. Samples were resolved by 5% polyacrylamide gel electrophoresis in 0.5% Tris-buffered EDTA at 300 V for 2 hours. The dried gels were exposed to a phosphorimager cassette (Amersham Biosciences) and were analyzed with Storm840 software (Amersham Biosciences). Oligonucleotide sequences for the HNF-4α site in the *Kir6.2* gene were as follows: forward, 5′-GGGGAAGGCCAGACCAAAGGGCAGACCCT-3′; reverse, 5′-GGGGAGGGTCTGCCCTTTGGTCTGGCCTT-3′.

Transient transfections and luciferase reporter assays. A 237-bp fragment of the *Kir6.2* promoter containing the putative HNF-4α binding site was cloned by PCR to contain *Kpn*I and *Bgl*II restriction enzyme sites on the 5′ and 3′ ends, respectively. A mutated version of this element was generated by overlap PCR (Figure 6D). The wild-type and mutant PCR fragments were then cloned into the *Kpn*I and *Bgl*II sites of the pGL3 promoter luciferase vector (Promega Corp.). The pCMVβ-HNF 4α plasmid (a kind gift from M. Stoffel, Rockefeller University, New York, New York, USA) was used to expresses FLAG-tagged HNF-4α under control of the cytomegalovirus promoter. BHK cells (5×10^5) were seeded 16 hours prior to transfection in 60-mm dishes and were cultured in DMEM supplemented with 10% FBS, L-glutamine, penicillin, and streptomycin. Transient transfections were performed using the Effectine transfection reagent (QIAGEN) according to the manufacturer's instructions. At 24 hours after transfection, cells were harvested and luciferase activity was measured using the Dual Luciferase Reporter Assay (Promega Corp.). Luciferase activity was normalized for transfection efficiency by the corresponding Renilla luciferase activity.

Acknowledgments

The authors are grateful to M.A. Lazar, D.A. Stoffers, and J.R. Friedman for critical reading of the manuscript. The authors thank Kristen A. Lantz, Sara D. Sackett, Regina K. Gorski, Maria Golson, John E. Brestelli, and Peter White for contributions to this work, and Shamina Rangwala and Phillip P. Le for valuable discussions. The authors are also grateful to Heather Collins for performing radioimmune assays, Nicolai Doliba for help with calcium-imaging experiments, and Harshani Peiris and Linda Greenbaum for liver nuclear extracts. Our studies were assisted by the University of Pennsylvania Diabetes Center (P30DK19525) and the Penn Center for Molecular Studies in Digestive and Liver Disease (P30DK50306). This work was supported by the National Institute of Diabetes and Digestive and Kidney Diseases (grants DK55342 and DK56947 to K.H. Kaestner; DK55743 and DK60064 to S.A. Duncan; and DK61226 to C.S. Lee).

Received for publication June 7, 2004, and accepted in revised form January 18, 2005.

Address correspondence to: Klaus H. Kaestner, Department of Genetics, University of Pennsylvania School of Medicine, 415 Curie Boulevard, Philadelphia, Pennsylvania 19104-6145, USA. Phone: (215) 898-8759; Fax: (215) 573-5892; E-mail:kaestner@mail.med.upenn.edu.

1. Shih, D.Q., and Stoffel, M. 2002. Molecular etiologies of MODY and other early-onset forms of diabetes. *Curr. Diab. Rep.* **2**:125–134.
2. Yamagata, K., et al. 1996. Mutations in the hepatocyte nuclear factor-1alpha gene in maturity-onset diabetes of the young (MODY3). *Nature.* **384**:455–458.
3. Gragnoli, C., et al. 1997. Maturity-onset diabetes of the young due to a mutation in the hepatocyte nuclear factor-4 alpha binding site in the promoter of the hepatocyte nuclear factor-1 alpha gene. *Diabetes.* **46**:1648–1651.
4. Silander, K., et al. 2004. Genetic variation near the hepatocyte nuclear factor-4 alpha gene predicts susceptibility to type 2 diabetes. *Diabetes.* **53**:1141–1149.
5. Love-Gregory, L.D., et al. 2004. A common polymorphism in the upstream promoter region of the hepatocyte nuclear factor-4 alpha gene on chromosome 20q is associated with type 2 diabetes and appears to contribute to the evidence for linkage in an ashkenazi jewish population. *Diabetes.* **53**:1134–1140.
6. Hansen, S.K., et al. 2002. Genetic evidence that HNF-1α–dependent transcriptional control of HNF-4α is essential for human pancreatic β cell function. *J. Clin. Invest.* **110**:827–833. doi:10.1172/JCI200215085.
7. Boj, S.F., Parrizas, M., Maestro, M.A., and Ferrer, J. 2001. A transcription factor regulatory circuit in differentiated pancreatic cells. *Proc. Natl. Acad. Sci. U. S. A.* **98**:14481–14486.
8. Servitja, J.M., and Ferrer, J. 2004. Transcriptional networks controlling pancreatic development and beta cell function. *Diabetologia.* **47**:597–613.
9. Ferrer, J. 2002. A genetic switch in pancreatic beta-cells: implications for differentiation and haploinsufficiency. *Diabetes.* **51**:2355–2362.
10. Wang, H., Maechler, P., Antinozzi, P.A., Hagenfeldt, K.A., and Wollheim, C.B. 2000. Hepatocyte nuclear factor 4alpha regulates the expression of pancreatic beta-cell genes implicated in glucose metabolism and nutrient-induced insulin secretion. *J. Biol. Chem.* **275**:35953–35959.
11. Odom, D.T., et al. 2004. Control of pancreas and liver gene expression by HNF transcription factors. *Science.* **303**:1378–1381.
12. Herman, W.H., et al. 1997. Diminished insulin and glucagon secretory responses to arginine in nondiabetic subjects with a mutation in the hepatocyte nuclear factor-4alpha/MODY1 gene. *Diabetes.* **46**:1749–1754.
13. Chen, W.S., et al. 1994. Disruption of the HNF-4 gene, expressed in visceral endoderm, leads to cell death in embryonic ectoderm and impaired gastrulation of mouse embryos. *Genes Dev.* **8**:2466–2477.
14. Duncan, S.A., Nagy, A., and Chan, W. 1997. Murine gastrulation requires HNF-4 regulated gene expression in the visceral endoderm: tetraploid rescue of Hnf-4(–/–) embryos. *Development.* **124**:279–287.
15. Postic, C., et al. 1999. Dual roles for glucokinase in glucose homeostasis as determined by liver and pancreatic beta cell-specific gene knock-outs using Cre recombinase. *J. Biol. Chem.* **274**:305–315.
16. Bonner-Weir, S. 1994. Regulation of pancreatic beta-cell mass in vivo. *Recent Prog. Horm. Res.* **49**:91–104.
17. Kulkarni, R.N., et al. 1999. Tissue-specific knockout of the insulin receptor in pancreatic beta cells creates an insulin secretory defect similar to that in type 2 diabetes. *Cell.* **96**:329–339.
18. Sund, N.J., et al. 2001. Tissue-specific deletion of Foxa2 in pancreatic beta cells results in hyperinsulinemic hypoglycemia. *Genes Dev.* **15**:1706–1715.
19. Duncan, S.A., et al. 1994. Expression of transcription factor HNF-4 in the extraembryonic endoderm, gut, and nephrogenic tissue of the developing mouse embryo: HNF-4 is a marker for primary endoderm in the implanting blastocyst. *Proc. Natl. Acad. Sci. U. S. A.* **91**:7598–7602.
20. Jiang, S., et al. 2003. Expression and localization of P1 promoter-driven hepatocyte nuclear factor-4α (HNF4α) isoforms in human and rats. *Nucl. Recept.* **1**:5.
21. Pontoglio, M., et al. 1998. Defective insulin secretion in hepatocyte nuclear factor 1α–deficient mice. *J. Clin. Invest.* **101**:2215–2222.
22. Shih, D.Q., et al. 2001. Loss of HNF-1alpha function in mice leads to abnormal expression of genes involved in pancreatic islet development and metabolism. *Diabetes.* **50**:2472–2480.
23. Johnson, J.D., et al. 2003. Increased islet apoptosis in *Pdx1*$^{+/-}$ mice. *J. Clin. Invest.* **111**:1147–1160. doi:10.1172/JCI200316537.
24. Bratanova-Tochkova, T.K., et al. 2002. Triggering and augmentation mechanisms, granule pools, and biphasic insulin secretion. *Diabetes.* **51**:S83–S90.
25. Lantz, K.A., et al. 2004. Foxa2 regulates multiple pathways of insulin secretion. *J. Clin. Invest.* **114**:512–520. doi:10.1172/JCI200421149.
26. Hayhurst, G.P., Lee, Y.H., Lambert, G., Ward, J.M., and Gonzalez, F.J. 2001. Hepatocyte nuclear factor 4alpha (nuclear receptor 2A1) is essential for maintenance of hepatic gene expression and lipid homeostasis. *Mol. Cell. Biol.* **21**:1393–1403.
27. Sugden, M.C., and Holness, M.J. 2004. Potential role of peroxisome proliferator-activated receptor-alpha in the modulation of glucose-stimulated insulin secretion. *Diabetes.* **53**:S71–S81.
28. Froguel, P., and Velho, G. 1999. Molecular genetics of maturity-onset diabetes of the young. *Trends Endocrinol. Metab.* **10**:142–146.
29. Wang, H., Maechler, P., Hagenfeldt, K.A., and Wollheim, C.B. 1998. Dominant-negative suppression of HNF-1alpha function results in defective insulin gene transcription and impaired metabolism-secretion coupling in a pancreatic beta-cell line. *EMBO J.* **17**:6701–6713.
30. MacDonald, M.J., and Kowluru, A. 1985. Evidence for calcium enhanced phosphorylation of pyruvate kinase by pancreatic islets. *Mol. Cell. Biochem.* **68**:107–114.
31. MacDonald, M.J., Kowluru, A., and Chang, C.M. 1985. Evidence for phosphorylation of pancreatic islet pyruvate kinase. *Metabolism.* **34**:600–603.
32. Nestorowicz, A., et al. 1997. A nonsense mutation in the inward rectifier potassium channel gene, Kir6.2, is associated with familial hyperinsulinism. *Diabetes.* **46**:1743–1748.
33. Thomas, P., Ye, Y., and Lightner, E. 1996. Mutation of the pancreatic islet inward rectifier Kir6.2 also leads to familial persistent hyperinsulinemic hypoglycemia of infancy. *Hum. Mol. Genet.* **5**:1809–1812.
34. Koster, J.C., et al. 2002. Hyperinsulinism induced by targeted suppression of beta cell KATP channels. *Proc. Natl. Acad. Sci. U. S. A.* **99**:16992–16997.
35. Li, L., Rojas, A., Wu, J., and Jiang, C. 2004. Disruption of glucose sensing and insulin secretion by ribozyme Kir6.2-gene targeting in insulin-secreting cells. *Endocrinology.* **145**:4408–4414.
36. Miki, T., et al. 1998. Defective insulin secretion and enhanced insulin action in KATP channel-deficient mice. *Proc. Natl. Acad. Sci. U. S. A.* **95**:10402–10406.
37. Miki, T., et al. 1997. Abnormalities of pancreatic islets by targeted expression of a dominant-negative KATP channel. *Proc. Natl. Acad. Sci. U. S. A.* **94**:11969–11973.
38. Seino, S., Iwanaga, T., Nagashima, K., and Miki, T. 2000. Diverse roles of K(ATP) channels learned from Kir6.2 genetically engineered mice. *Diabetes.* **49**:311–318.
39. Seghers, V., Nakazaki, M., DeMayo, F., Aguilar-Bryan, L., and Bryan, J. 2000. Sur1 knockout mice. A model for K(ATP) channel-independent regulation of insulin secretion. *J. Biol. Chem.* **275**:9270–9277.
40. Miki, T., et al. 2002. ATP-sensitive potassium channels participate in glucose uptake in skeletal muscle and adipose tissue. *Am. J. Physiol. Endocrinol. Metab.* **283**:E1178–E1184.
41. Remedi, M.S., et al. 2004. Diet-induced glucose Intolerance in mice with decreased β-cell ATP-sensitive K^+ channels. *Diabetes.* **53**:3159–3167.
42. Li, C., et al. 2004. A signaling role of glutamine in insulin secretion. *J. Biol. Chem.* **279**:13393–13401.
43. Doliba, N.M., et al. 2004. Restitution of defective glucose-stimulated insulin release of sulfonylurea type 1 receptor knockout mice by acetylcholine. *Am. J. Physiol. Endocrinol. Metab.* **286**:E834–E843.
44. Prentki, M., Joly, E., El-Assaad, W., and Roduit, R. 2002. Malonyl-CoA signaling, lipid partitioning, and glucolipotoxicity: role in beta-cell adaptation and failure in the etiology of diabetes. *Diabetes.* **51**:S405–S413.
45. Deeney, J.T., Prentki, M., and Corkey, B.E. 2000. Metabolic control of beta-cell function. *Semin. Cell Dev. Biol.* **11**:267–275.
46. Shih, D.Q., et al. 2000. Genotype/phenotype relationships in HNF-4alpha/MODY1: haploinsufficiency is associated with reduced apolipoprotein (AII), apolipoprotein (CIII), lipoprotein(a), and triglyceride levels. *Diabetes.* **49**:832–837.
47. Parviz, F., et al. 2003. Hepatocyte nuclear factor 4alpha controls the development of a hepatic epithelium and liver morphogenesis. *Nat. Genet.* **34**:292–296.
48. Nishigori, H., et al. 1998. Frameshift mutation, A263fsinsGG, in the hepatocyte nuclear factor-1beta gene associated with diabetes and renal dysfunction. *Diabetes.* **47**:1354–1355.
49. Wang, L., et al. 2004. Selective deletion of the HNF1β (MODY5) gene in β-cells leads to altered gene expression and defective insulin release. *Endocrinology.* **145**:3941–3949.
50. Parviz, F., Li, J., Kaestner, K.H., and Duncan, S.A. 2002. Generation of a conditionally null allele of HNF4alpha. *Genesis.* **32**:130–133.
51. Scharp, D.W., Kemp, C.B., Knight, M.J., Ballinger, W.F., and Lacy, P.E. 1973. The use of Ficoll in the preparation of viable islets of Langerhans from the rat pancreas. *Transplantation.* **16**:686–689.
52. Li, C., et al. 2003. Regulation of leucine-stimulated insulin secretion and glutamine metabolism in isolated rat islets. *J. Biol. Chem.* **278**:2853–2858.
53. Lee, C.S., et al. 2002. Foxa2 controls Pdx1 gene expression in pancreatic beta-cells in vivo. *Diabetes.* **51**:2546–2551.
54. Podvinec, M., Kaufmann, M.R., Handschin, C., and Meyer, U.A. 2002. NUBIScan, an in silico approach for prediction of nuclear receptor response elements. *Mol. Endocrinol.* **16**:1269–1279.
55. Ellrott, K., Yang, C., Sladek, F.M., and Jiang, T. 2002. Identifying transcription factor binding sites through Markov chain optimization. *Bioinformatics.* **18**:S100–S109.